Electronic Supplementary Material (ESI) for Journal of Materials Chemistry A.

Supplemental Information for

Stability of push-pull small molecule donors for organic photovoltaics: spectroscopic degradation of acceptor endcaps on benzo[1,2-b: 4,5-b’] dithiophene cores

Kristen E. Watts,[a‡] Trung Nguyen,[b‡] Bertrand J. Tremolet de Villers,[c] Bharati Neelamraju,[b] Michael A. Anderson,[b] Wade A. Braunecker,[c] Andrew J. Ferguson,[c] Ross E. Larsen,[d] Bryon W. Larson,[c] Zbyslaw R. Owczarczyk,[c] Jason R. Pfeilsticker,[c] Jeanne E. Pemberton,[a*] Erin L. Ratcliff[b,e*]

[a] Department of Chemistry and Biochemistry, University of Arizona, Tucson, AZ, 85721.
[b] Department of Materials Science and Engineering, University of Arizona, Tucson, AZ, 85721.
[c] Chemistry and Nanoscience Center, National Renewable Energy Laboratory, Golden, CO, 80401.
[d] Computational Science Center, National Renewable Energy Laboratory, Golden, CO, 80401.
[e] Department of Chemical and Environmental Engineering, University of Arizona, Tucson, AZ, 85721.
[‡] Authors contributed equally to this publication.

* pembertn@email.arizona.edu, ratcliff@email.arizona.edu

1. Synthesis

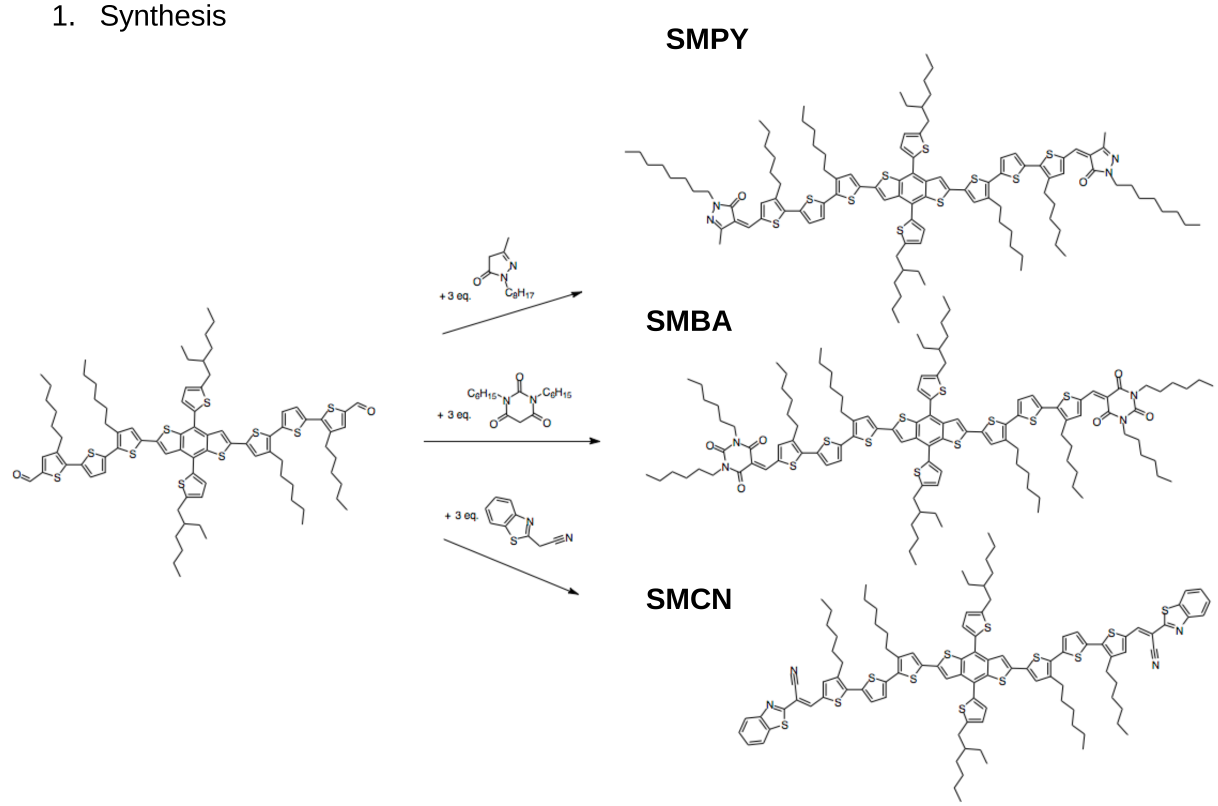

Scheme S1. Synthesis of SMPy (top), SMBA (middle), and SMCN (bottom).

1-*n*-octyl-3-methyl-5-pyrazolone was synthesized according to a literature procedure [1] as was the dicarbaldehyde precursor in **Scheme S1**. [2]

SMPY. This compound was prepared by dissolving 146 mg (0.1 mmol) of the dicarbaldehyde precursor in 5 mL of THF with 63 mg (0.30 mmol) 1-*n*-octyl-3-methyl-5-pyrazolone. 3 μL of tetramethylguanidine was added to the solution, and it was stirred overnight at 60 °C under nitrogen. The THF was removed with a rotary evaporator, and after washing the crude product with acetone, it was purified by column chromatography (chloroform:hexane = 9:1) to give ~90 mg of the product (~48% yield) as a purple solid.

^{1}H NMR (400 MHz, $CDCl_3$): δ 7.77 (s, 2H), 7.59 (s, 2H), 7.31 (m, 6H), 7.10 (d, *J* = 4 Hz, 2H), 7.08 (s, 2H), 6.93 (d, *J* = 4 Hz, 2H), 3.74 (t, *J* = 7.6 Hz, 4H), 2.90 (m, 4H), 2.83 (t, *J* = 8 Hz, 4H), 2.75 (t, *J* = 8 Hz, 4H), 1.70 (m, 16H), 1.25 – 1.50 (m, 64H), 0.85 – 1.00 (m, 30H).

^{13}C NMR (100 MHz, $CDCl_3$): δ163.63, 148.58, 146.55, 144.28, 144.03, 141.52, 140.79, 139.22, 138.53, 137.95, 137.88, 137.33, 136.13, 135.63, 135.42, 134.74, 131.08, 128.89, 128.49, 128.41, 128.38, 126.77, 126.02, 123.89, 122.14, 119.71, 44.76, 42.03, 34.92, 33.09, 32.32, 32.21, 32.19, 30.90, 30.73, 30.25, 29.95, 29.84, 29.81, 29.80, 29.72, 29.51, 29.27, 27.38, 26.39, 23.59, 23.16, 23.14, 14.74, 13.41, 11.51.

Elemental analysis calcd (%) for $C_{108}H_{142}N_4O_2S_{10}$: C 69.32, H 7.63, N 2.53; found: C 69.55, H 7.75, N 2.96. HRMS m/z: $[M + H]^+$ calcd for $C_{108}H_{143}N_4O_2S_{10}$: 1848.8452, found 1848.8406.

SMCN. This compound was prepared in an analogous manner to SMPY by dissolving 146 mg (0.1 mmol) of dicarbaldehyde precursor in 5 mL of THF with 52 mg (0.30 mmol) 2-benzothiazoleacetonitrile. After reaction workup, the crude product was purified by column chromatography (chloroform:hexane = 9:1) to give ~97 mg of the product (~55% yield) as a purple solid.

^{1}H NMR (400 MHz, $CDCl_3$): δ 8.15 (s, 2H), 7.98 (dd, 2H), 7.80 (dd, 2H), 7.51 (s, 2H), 7.60-7.30 (m, 8H), 7.23- 6.90 (m, 8H), 3.0-2.6 (m, 12H), 1.80 – 1.20 (m, 48H), 1.00 - 0.80 (m, 24H).

^{13}C NMR (100 MHz, $CDCl_3$): δ 163.16, 154.17, 146.40, 141.31, 140.72, 140.33, 139.58, 139.08, 138.54, 138.42, 137.76, 137.74, 137.37, 136.04, 135.40, 134.96, 130.94, 128.75, 128.37, 128.34, 128.22, 127.27, 126.45, 126.00, 125.96, 123.72, 123.63, 122.09, 122.04, 121.25, 119.59, 117.35, 101.06, 42.02, 34.92, 33.10, 32.21, 32.19, 30.82, 30.62, 30.05, 29.89, 29.78, 29.50, 26.38, 23.60, 23.18, 23.15, 14.74, 14.60, 11.51.

Elemental analysis calcd (%) for $C_{102}H_{110}N_4S_{12}$: C 68.95, H 6.24, N 3.15; found: C 68.60, H 6.28, N 3.28. $[M + H]^+$ calcd for $C_{102}H_{111}N_4S_{12}$: 1776.5491, found 1776.7244.

1,3-dihexylpyrimidine-2,4,6(1*H*,3*H*,5*H*)-trione. A modified literature procedure was used to synthesize alkylated barbituric acid compounds. [3] To a solution of *n*-hexyl amine (1.315 mL, 10.0 mmol) in 50 mL anhydrous dichloromethane was added a solution of *n*-hexyl isocyanate (1.27 g, 10.0 mmol) in 50 mL dichloromethane under nitrogen. After 1 h of stirring at rt, malonyl chloride (0.97 mL, 10.0 mmol) was added, and the mixture was stirred overnight at rt. The mixture was poured into water and extracted with ethyl acetate (2 x 50 mL). The organic phase was dried over $MgSO_4$, after which the ethyl acetate was removed on a rotary evaporator. The crude product was purified by column chromatography (hexane:ethyl acetate = 3:1) to give a yellow oil (1.50 g, 50% yield).

^{1}H NMR (400 MHz, $CDCl_3$): δ 3.87 (d, *J* = 7.6 Hz, 2H), 3.86 (d, *J* = 7.6 Hz, 2H), 3.66 (s, 2H), 1.59 (m, 4H), 1.32 (m, 12H), 0.90 (t, *J* = 7.0 Hz, 6H).

^{13}C NMR (100 MHz, $CDCl_3$): δ 164.57, 151.36, 42.09, 39.67, 31.67, 27.91, 26.46, 22.51, 13.98.

SMBA. This compound was prepared in an analogous manner to SMPY by dissolving 146 mg (0.1 mmol) of dicarbaldehyde precursor in 5 mL of THF with 106 mg (0.30 mmol) 1,3-dihexylpyrimidine-2,4,6(1*H*,3*H*,5*H*)-trione. After reaction workup, the crude product was purified by column chromatography (chloroform:hexane = 9:1) to give ~90 mg of the product (~45% yield) as a purple solid.

^{1}H NMR (400 MHz, $CDCl_3$): δ 8.52 (s, 2H), 7.62 (s, 2H), 7.60 (s, 2H), 7.41 (d, *J* = 4 Hz, 2H), 7.32 (d, *J* = 4 Hz, 2H), 7.13 (d, *J* = 4 Hz, 2H), 7.10 (s, 2H), 6.93 (d, *J* = 4 Hz, 2H), 3.96 (m, 8H), 2.90 (m, 4H), 2.82 (t, *J* = 8 Hz, 4H), 2.76 (t, *J* = 8 Hz, 4H), 1.66 (m, 18H), 1.25 – 1.50 (m, 64H), 0.85 – 1.00 (m, 64H).

^{13}C NMR (100 MHz, $CDCl_3$): δ 163.05, 162.2, 151.46, 148.73, 148.48, 148.22, 146.59, 141.77, 140.73, 139.38, 139.25, 137.91, 137.28, 136.36, 135.33, 134.74, 130.92, 129.08, 128.93, 128.38, 126.84, 126.02, 123.92, 119.79, 110.07, 42.82, 42.08, 42.02, 34.89, 33.11, 33.07, 32.17, 32.04, 31.98, 30.88, 30.53, 30.28, 29.82, 29.8, 29.7, 29.49, 28.63, 28.54, 27.15, 27.08, 26.38, 23.58, 23.12, 23.06, 14.72, 14.58, 14.55, 14.53, 11.49.

Elemental analysis calcd (%) for $C_{116}H_{154}N_4O_6S_{10}$: C 68.93, H 7.68, N 2.77; found: C 68.64, H 7.75, N 2.78. HRMS m/z: $[M + H]^+$ calcd for $C_{116}H_{155}N_4O_6S_{10}$: 2020.9187, found found 2020.9018.

2. ^{1}H NMR (400 MHz, CDCl$_3$), ^{13}C NMR (100 MHz CDCl$_3$), and elemental anaysis for SMBA precursor and final products SMPy, SMCN, and SMBA.

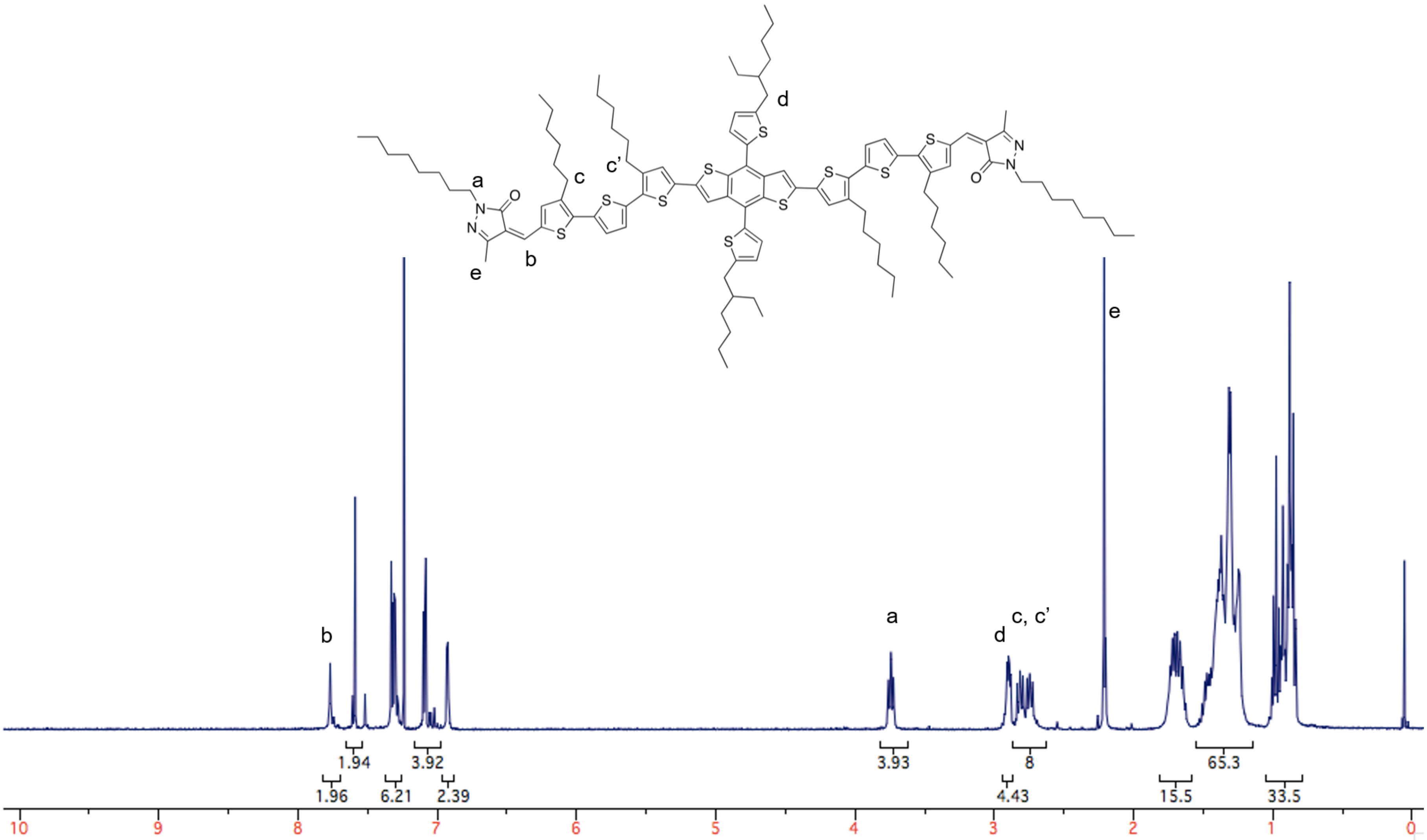

Figure S1. ^{1}H NMR of SMPy with key proton groups assigned.

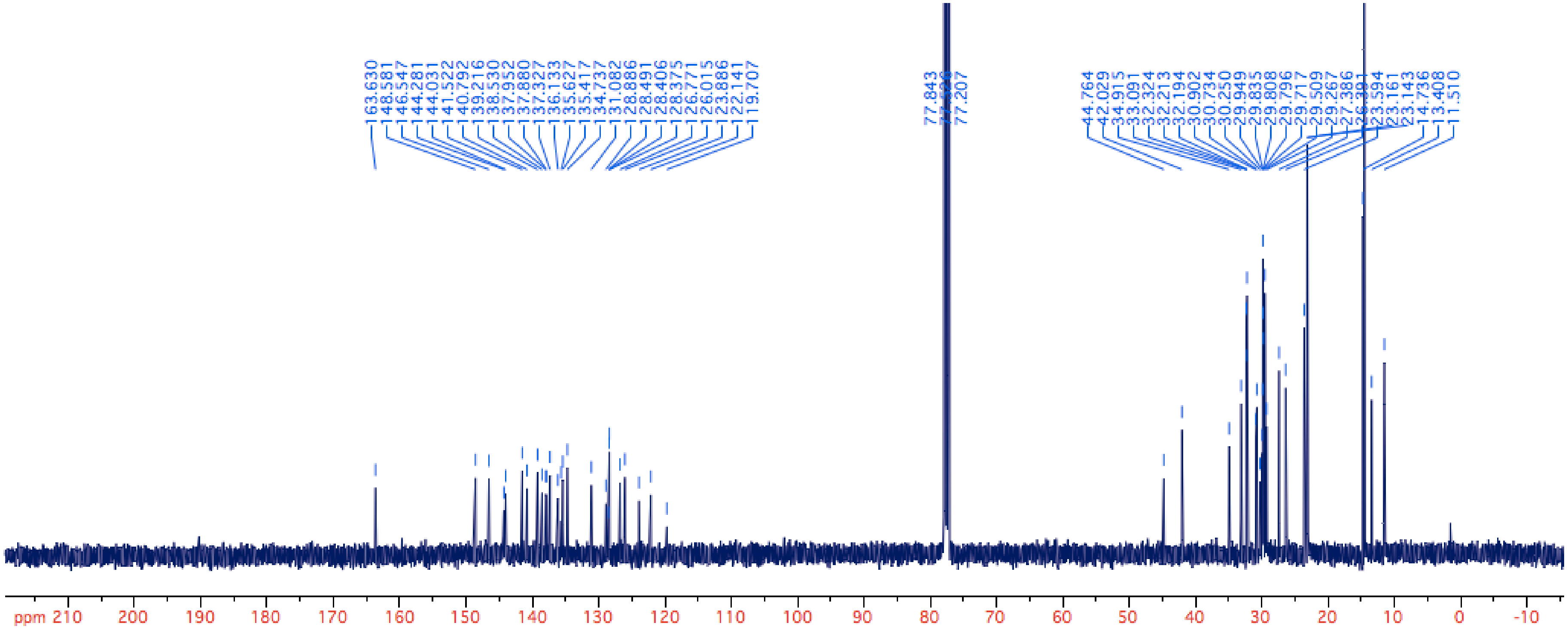

Figure S2. ^{13}C NMR spectra of SMPy in room temperature $CDCl_3$.

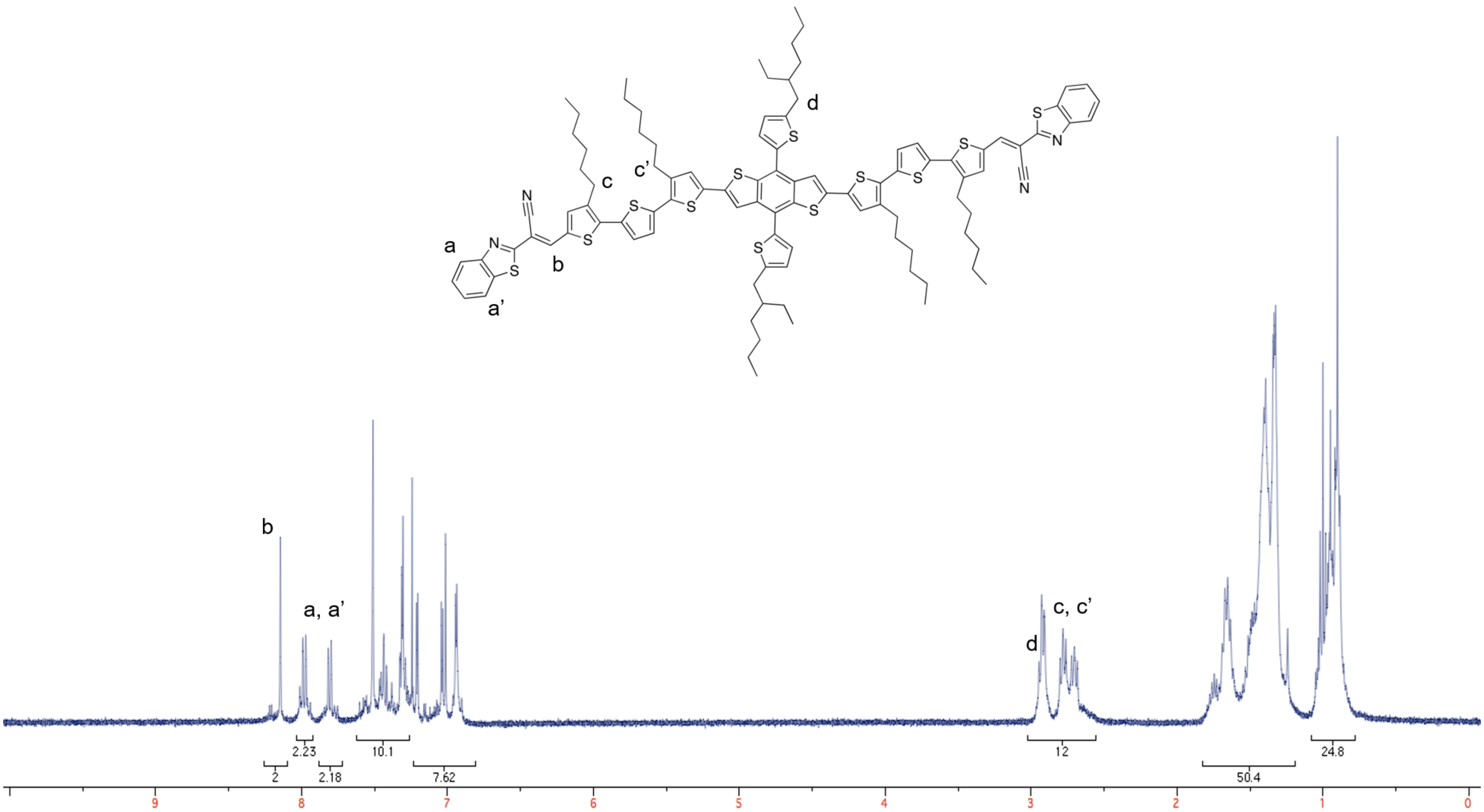

Figure S3. 1H NMR of SMCN with key proton groups assigned.

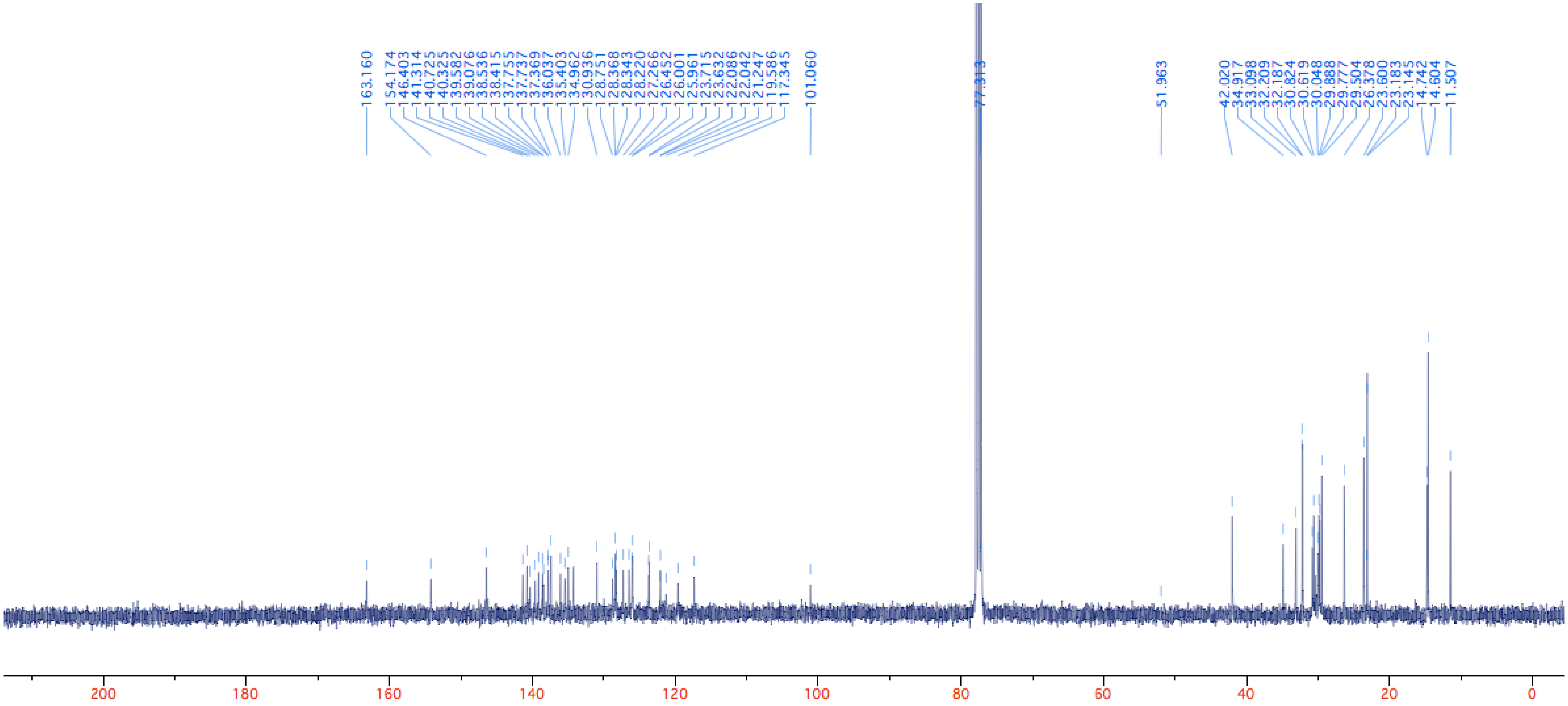

Figure S4. ^{13}C NMR spectra of SMCN in room temperature $CDCl_3$.

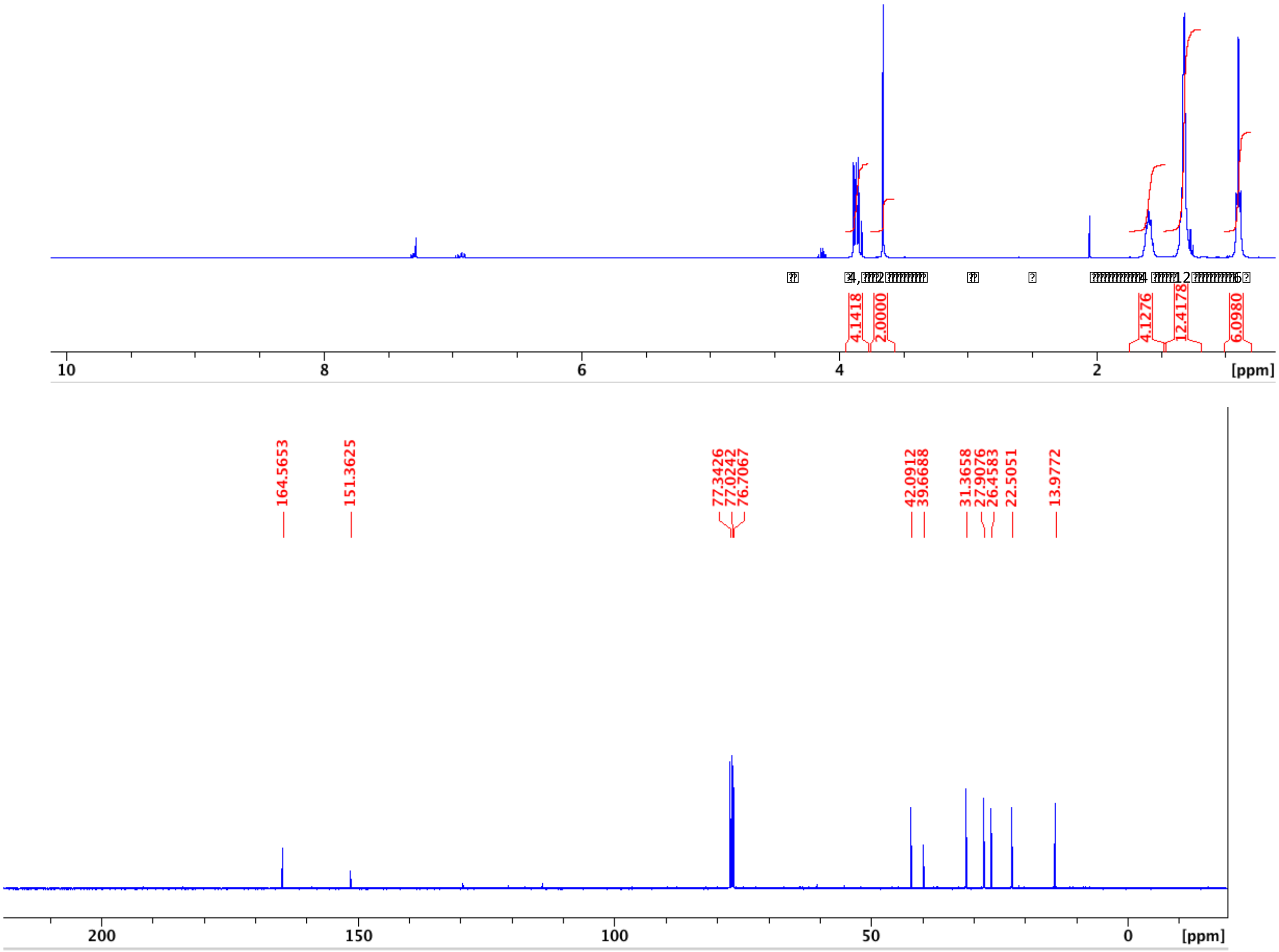

Figure S5. ^{1}H NMR and ^{13}C NMR spectra of 1,3-dihexylpyrimidine-2,4,6(1*H*,3*H*,5*H*)-trione in room temperature $CDCl_3$ (precursor for SMBA synthesis).

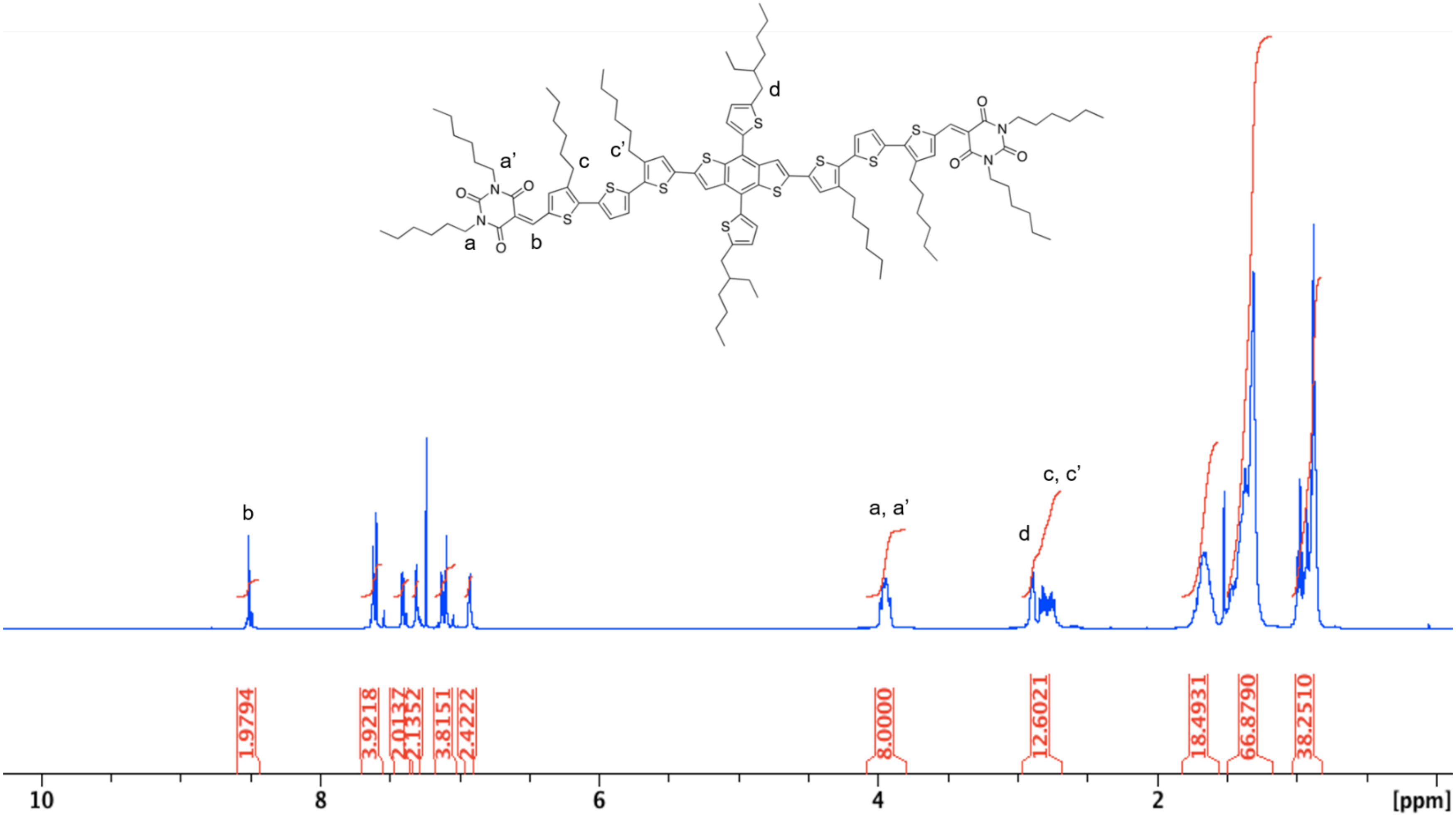

Figure S6. ^{1}H NMR of SMBA with key proton groups assigned.

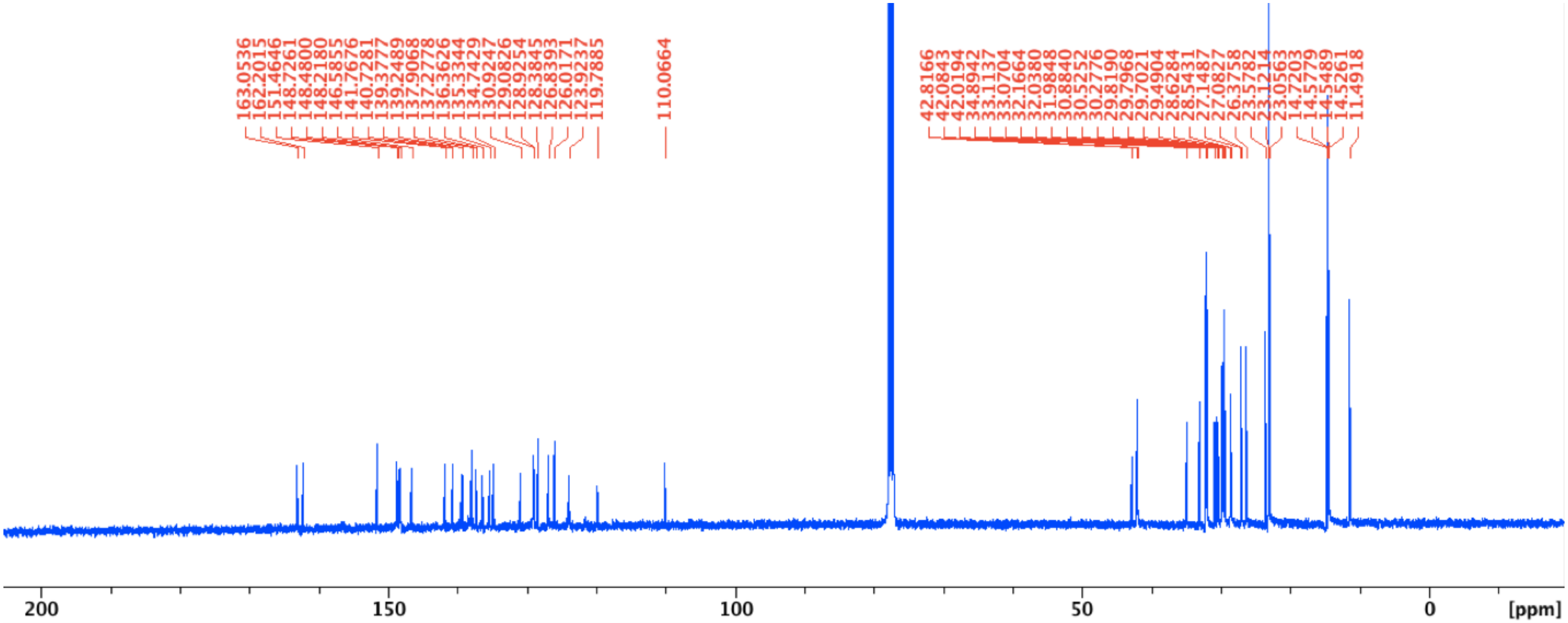

Figure S7. ^{13}C NMR spectra of SMBA in room temperature $CDCl_3$.

3. Laser Desorption Ionization Mass Spectrometry

Data for laser desorption ionization mass spectrometry analysis were collected on a 7T Fourier transform ion cyclotron resonance mass spectrometer (FT-ICR-MS, SolariX XR, Bruker, Bremen, Germany). The mass resolving power (m/Δm 50%) was at least 100,000 at m/z 400 during calibration. The sample dissolved in organic solvent (DCM) at approximately 0.1 wt% concentration was spotted at 2 uL on a ground stainless steel MTP 384 MALDI target plate (#8280784, Bruker). Laser ionization was initiated with a Nd:YAG laster, 355 nm, set at between 12 and 60% relative laser power and < 50 um beam diameter. Because these products are naturally light absorbing, no matrix was needed to obtain a highly sensitive signal. Mass spectra were collected in positive ion mode and 50 time domain transient scans were co-added for each sample prior to fast Fourier transformation and frequency to m/z conversion. The mass spectrometer was internally calibrated to achieve sub-part-per-million mass measurement accuracy on NaTFA in positive ion mode (-0.086 ppm at m/z 702.863262 m/z; 0.138 ppm at m/z 1246.762494) and tuned for m/z 100-2200 detection, at 0.7 ms ion time of flight in transfer optics.

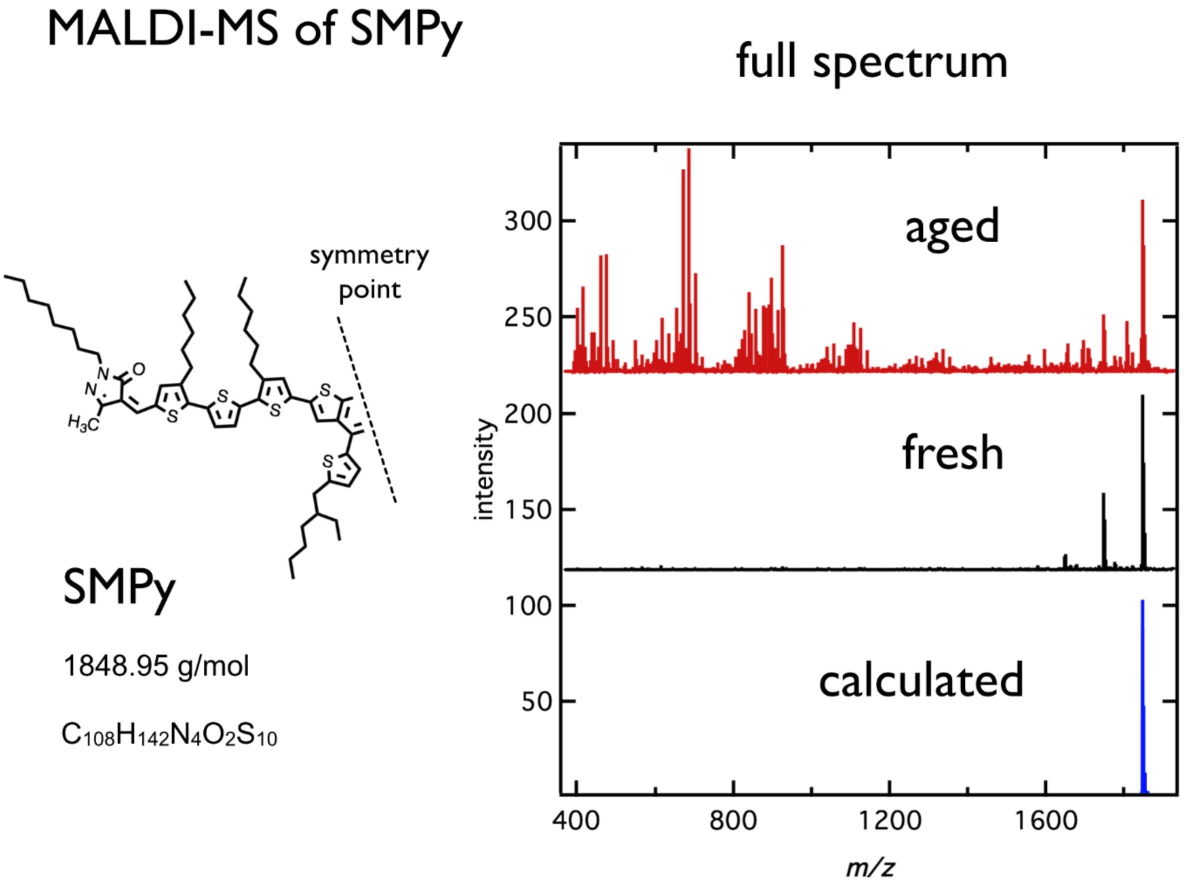

Figure S8. MALDI mass spectra for SMPy

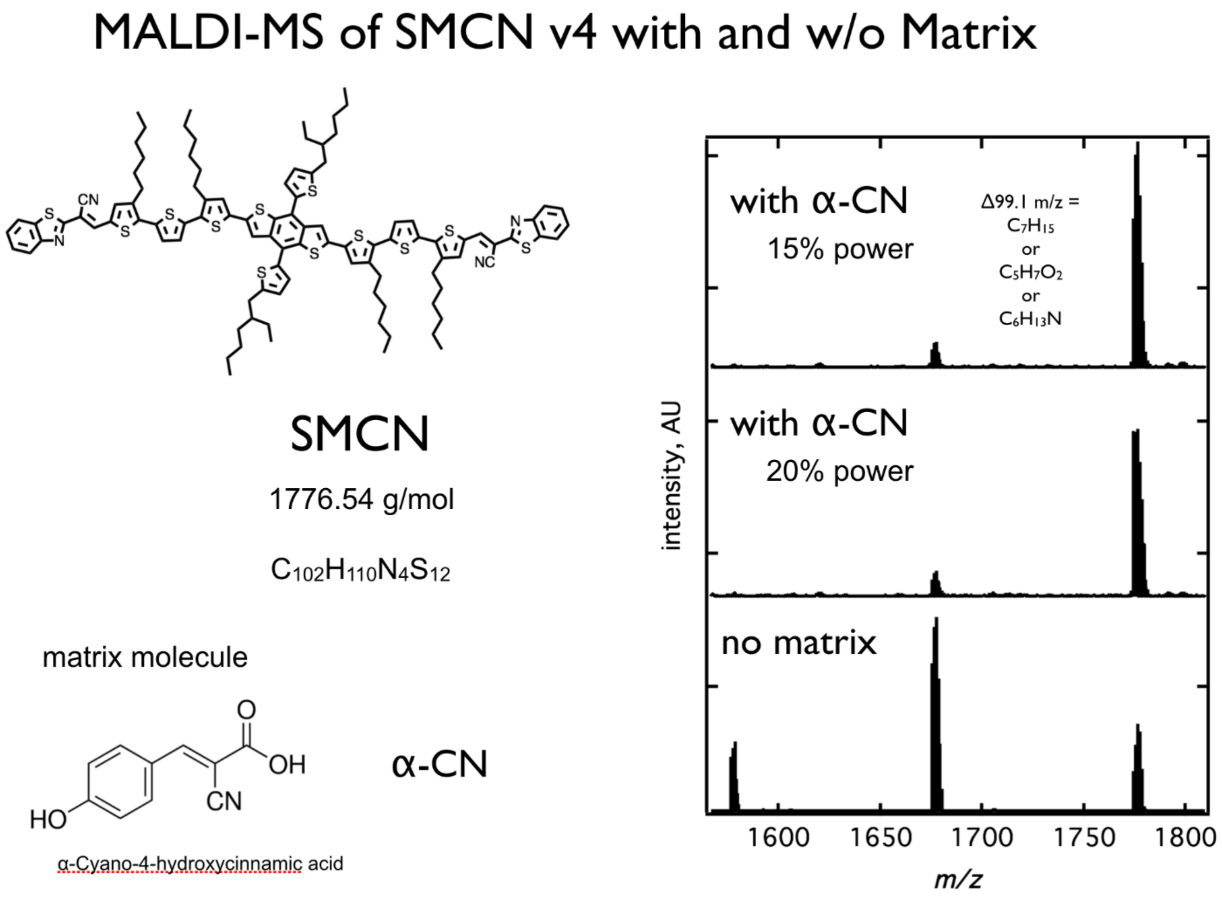

Figure S9. MALDI mass spectra for SMCN.

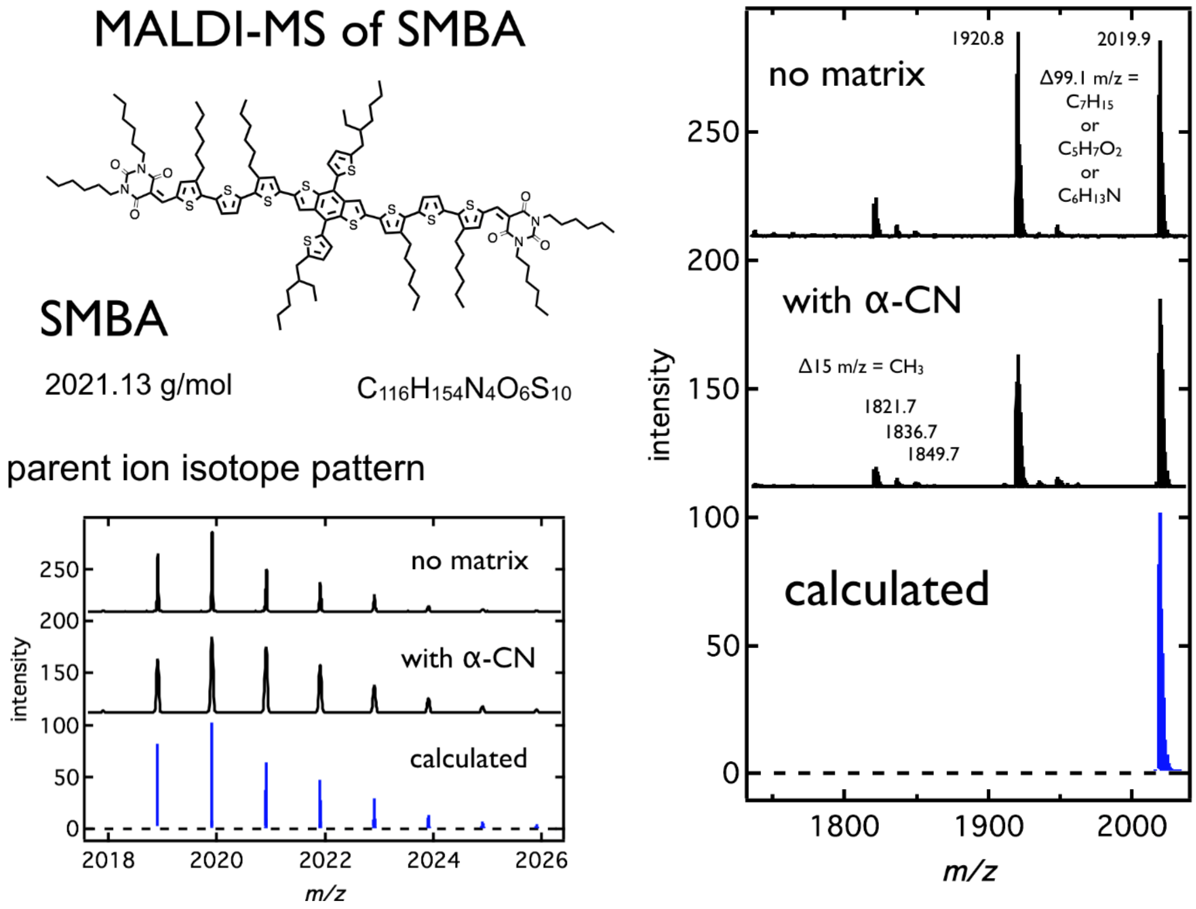

Figure S10. MALDI mass spectra for SMBA

4. Contour plots of molecular orbitals for SMPy and SMBA

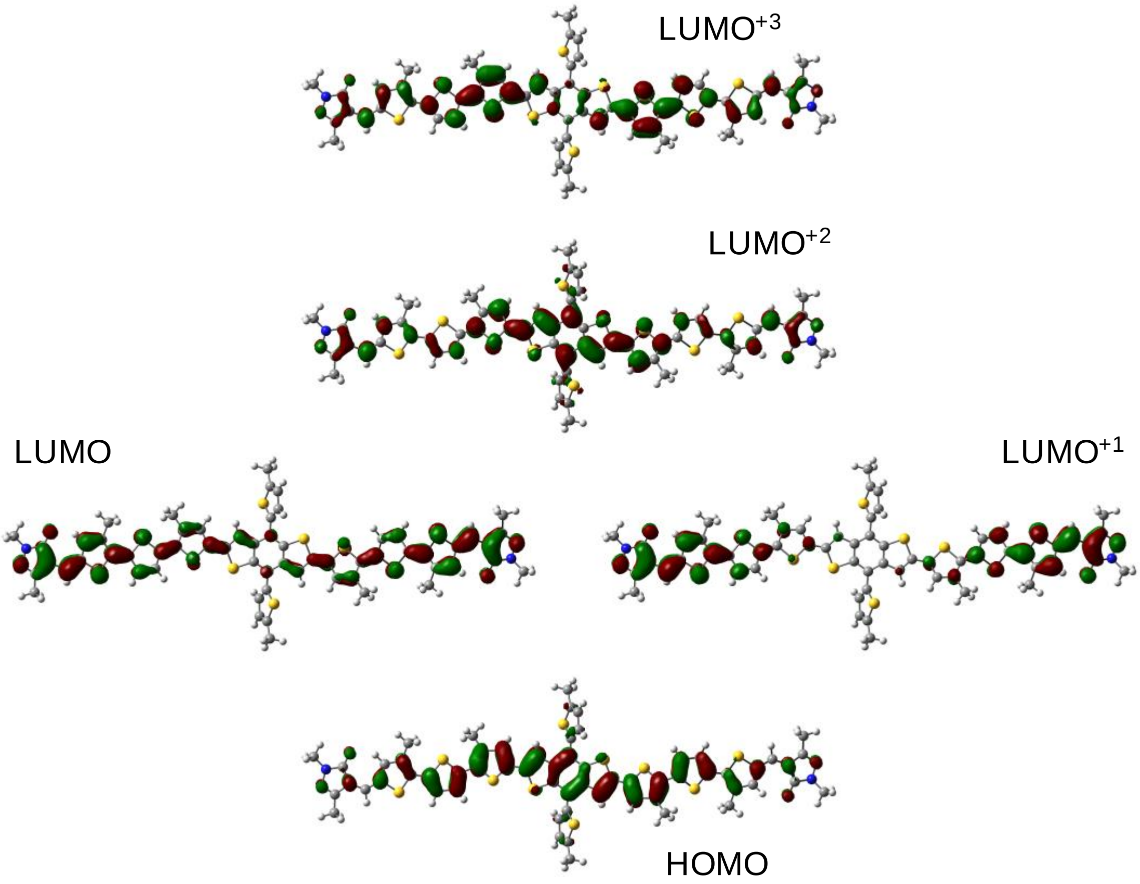

Figure S11. Contour plots of Kohn-Sham molecular orbitals of SMPy calculated with DFT as described in the main text. Displayed are the HOMO, LUMO, LUMO^{+1}, LUMO^{+2} and LUMO^{+3} levels for contours at ±0.02 a.u.

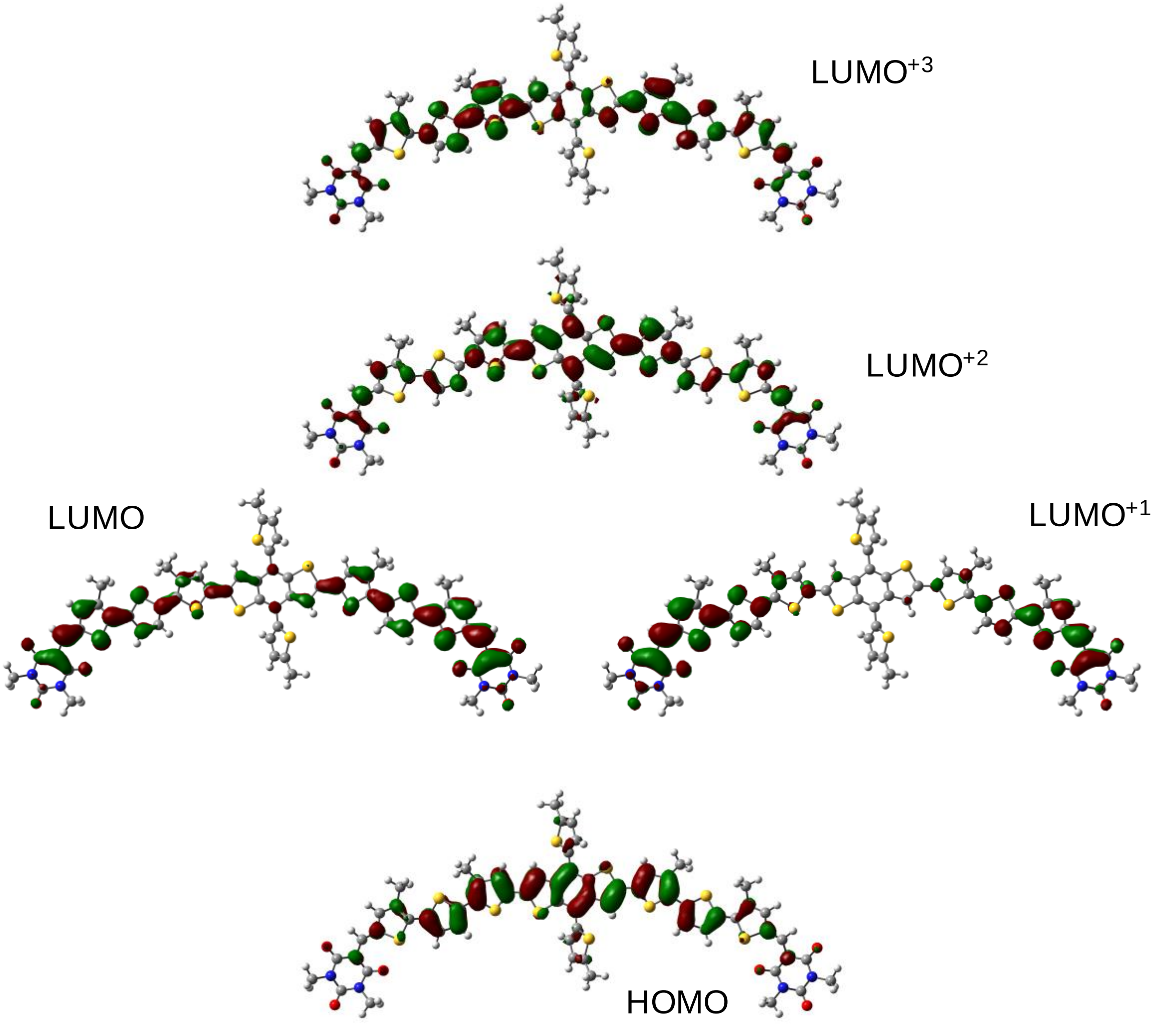

Figure S12. Contour plots of Kohn-Sham molecular orbitals of SMBA calculated with DFT as described in the main text. Displayed are the HOMO, LUMO, LUMO^{+1}, LUMO^{+2} and LUMO^{+3} levels for contours at ±0.02 a.u.

5. Characterization of photodegradation experiment and testing environment statistics

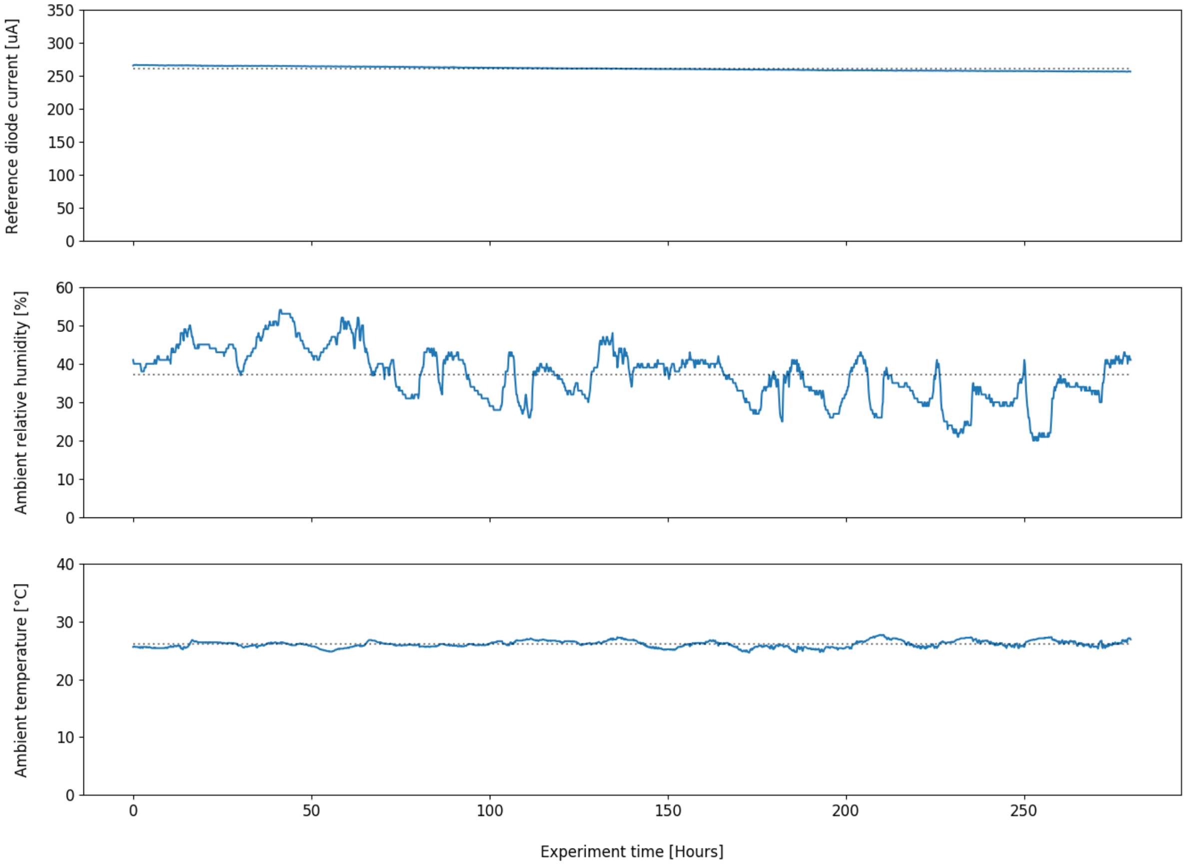

Figure S13. Plots showing the stability of the light source (top), minor fluctuations in ambient relative humidity (center), and stability of ambient temperature over the course of the time dependent photobleaching studies conducted on the four molecules. Dotted lines indicate average value over monitored time.

The statistics on the testing environment data are as follows:

Degradation lamp reference diode current percent Change = -3.4 %
Average degradation lamp reference diode current = 261.0 uA
Degradation lamp reference diode current min, max = 256.0 uA, 266.4 uA
Degradation lamp reference diode current standard deviation = 6.9 uA
Degradation lamp reference diode current COV% = 1.197 %

Average relative humidity = 37.133 %
Relative humidity min, max = 20.0 %, 54.0 %
Relative humidity standard deviation = 6.907 %
Relative humidity COV% = 18.6 %

Average temperature = 26.084 °C
Temperature min, max = 24.6 °C, 27.7 °C
Temperature standard deviation = 0.579 °C
Temperature COV% = 2.218 %

6. Additional Uv-vis absorbance measurements

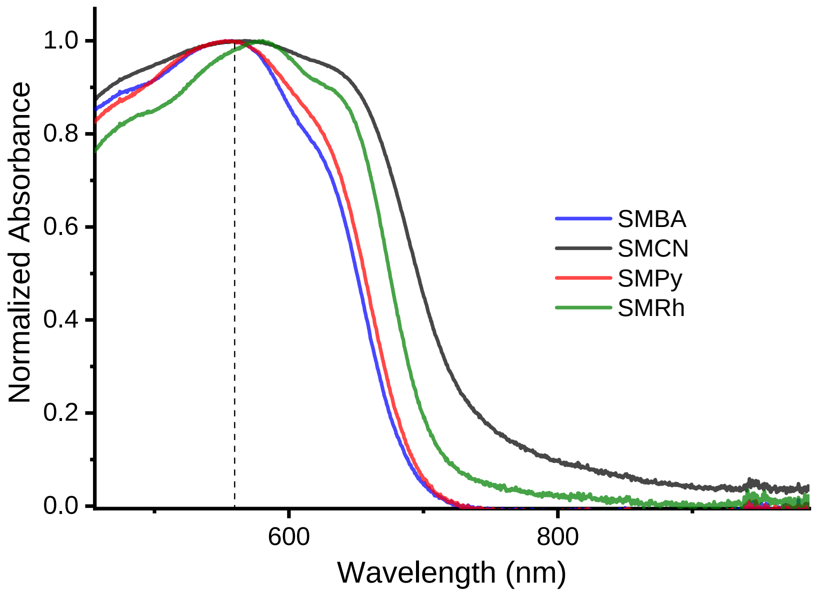

Figure S14. UV-Vis absorption spectra of all SMBA, SMCN, SMPy, and SMRh normalized to their λ_{max} values at 557.5, 568, 553, 580.5 nm, respectively

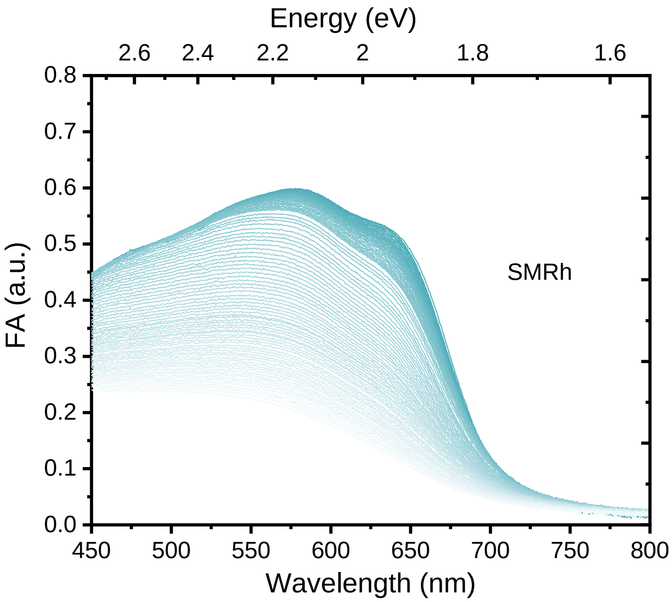

Figure S15. UV-Vis absorptance (FA) spectra taken over a period of 11 days for SMRh.

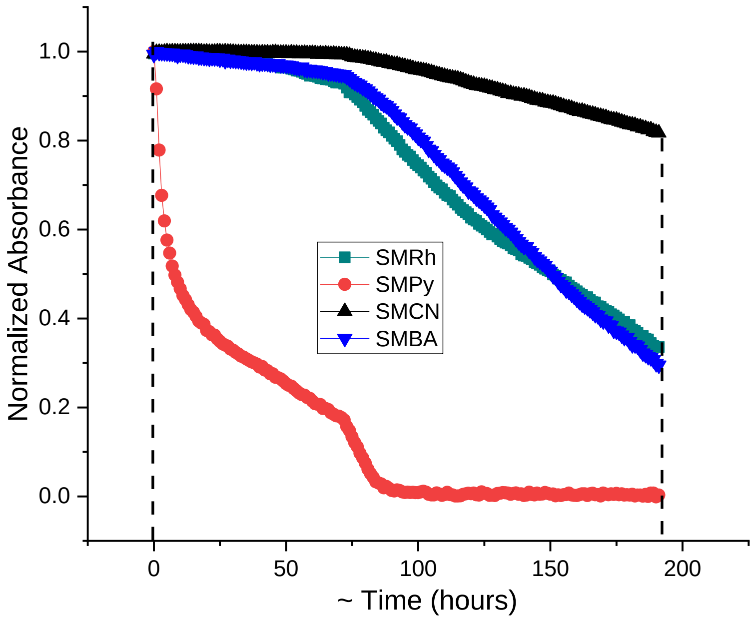

Figure S16. Trend in UV-vis peak absorbance change at λ_{max} for all the 4 molecules as they are photo bleached from t = 0 to t = 11 days.

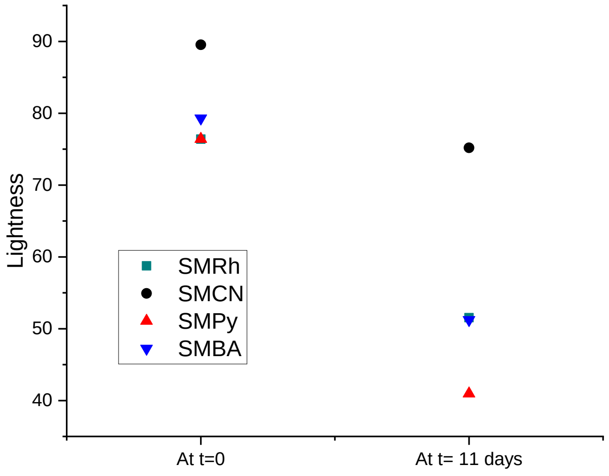

Figure S17. Lightness values calculated from the CIE L*a*b* coordinate system for the 4 molecules at t=0 as pristine films and t=11days as degraded films.

7. Time-dependent FTIR

Fourier Transform Infrared Spectroscopy (FTIR) was collected using a Thermo Scientific Nicolet 6700 spectrometer with a liquid nitrogen cooled MCT/A detector. Scan resolution was approximately 1 cm^{-1} and the average of 128 scans was recorded. Films of small molecules were deposited by drop-casting from solution onto Real Crystal IR sample cards with 19 mm-diameter KBr windows (International Crystal Laboratories). From time to time, the films were removed from the photo-bleaching setup described in the main text and the FTIR spectrum was measured in transmission mode. For each set of spectra for a given molecule, a high-order (n>4) polynomial equation was used to make a baseline fit to the first spectrum in the time series; and then that fit was applied to each spectrum in the dataset.

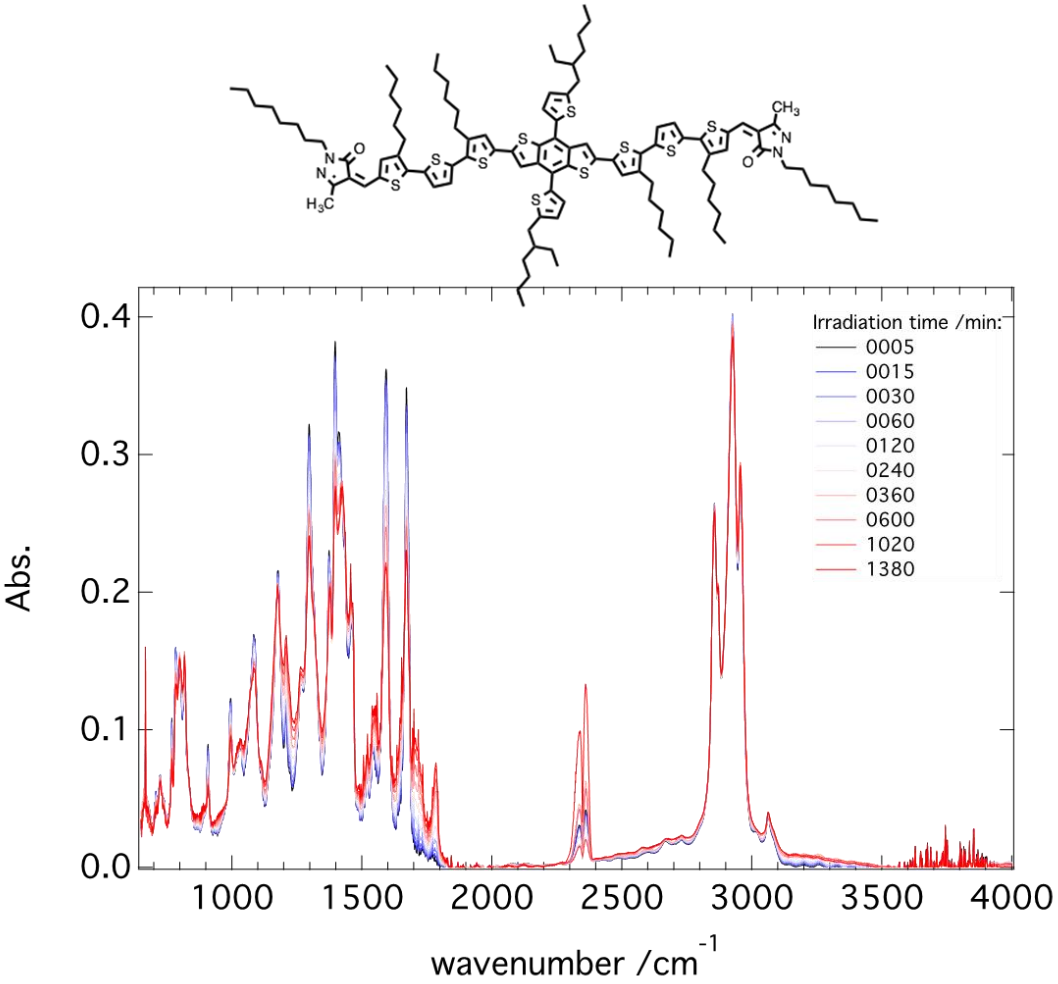

Figure S18. Time-dependent FTIR spectra of a photo-bleached SMPy film: No major changes are observed in the region of methyl and methylene stretches, 2800-3100cm^{-1}, indicating side-chain stability. There are significant changes with light exposure to vibrational absorptions attributed to the pyrazolone end group, including the carbonyl stretch around 1670cm^{-1} and the C=N mode around 1600cm^{-1}, confirming the ring-opening mechanisms proposed in the main text. Additionally, at longer light exposure times, we observe the emergence of peaks at 1210cm^{-1} and 1050cm^{-1}, suggestive of oxidation of sulfur atoms in the BDT-3T unit into sulfone and sulfoxide, respectively.

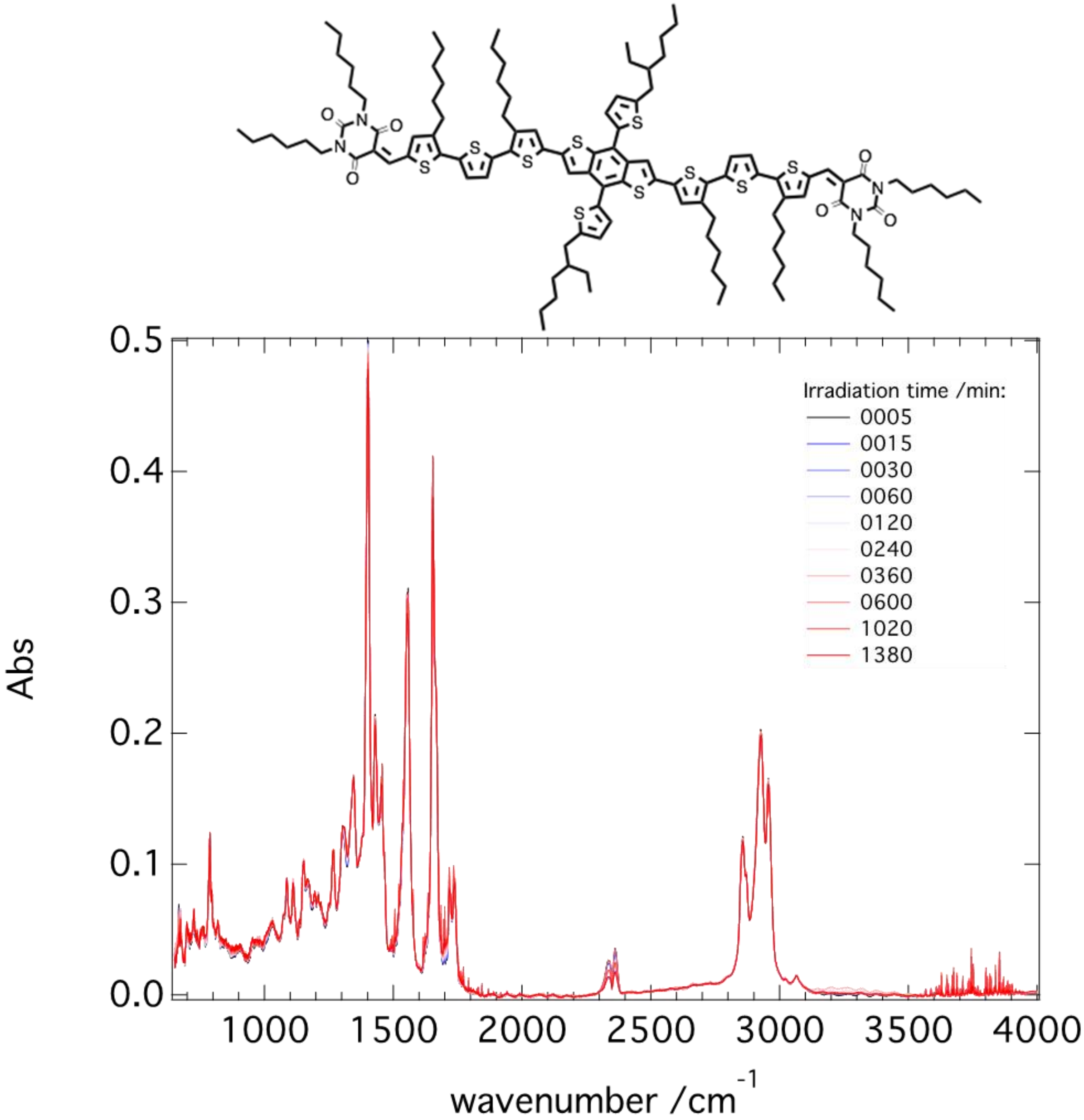

Figure S19. Time-dependent FTIR spectra of a photo-bleached SMBA film: The SMBA spectra show little change with light exposure. Unchanging absorptions from the carbonyl vibrations of -N-CO-N-, 1735cm^{-1} and 1715cm^{-1}, and from -C-CO-N- at 1653cm^{-1}, indicate that the barbituric end group is stable in this sample.

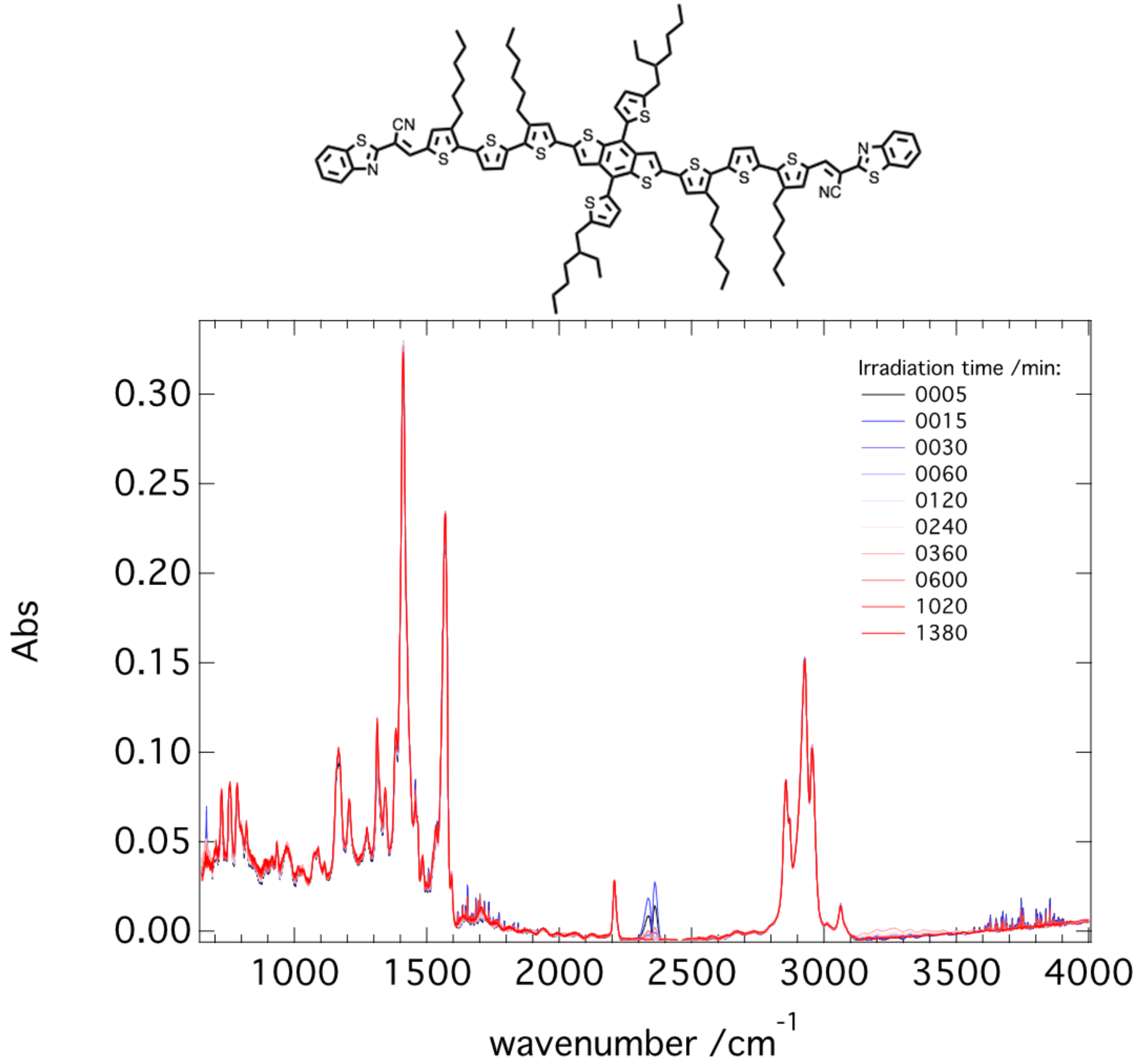

Figure S20. Time-dependent FTIR spectra of a photo-bleached SMCN film: Like SMBA, the FTIR spectra of SMCN are constant. Vibrational absorptions of the -CN at 2208cm^{-1} and of the -C=N in the thiazole ring at 1593cm^{-1} do not change with light exposure. SMCN appears stable to photo-bleaching.

8. C, N K-edge and S L-edge of SMPY, SMBA, and SMCN.

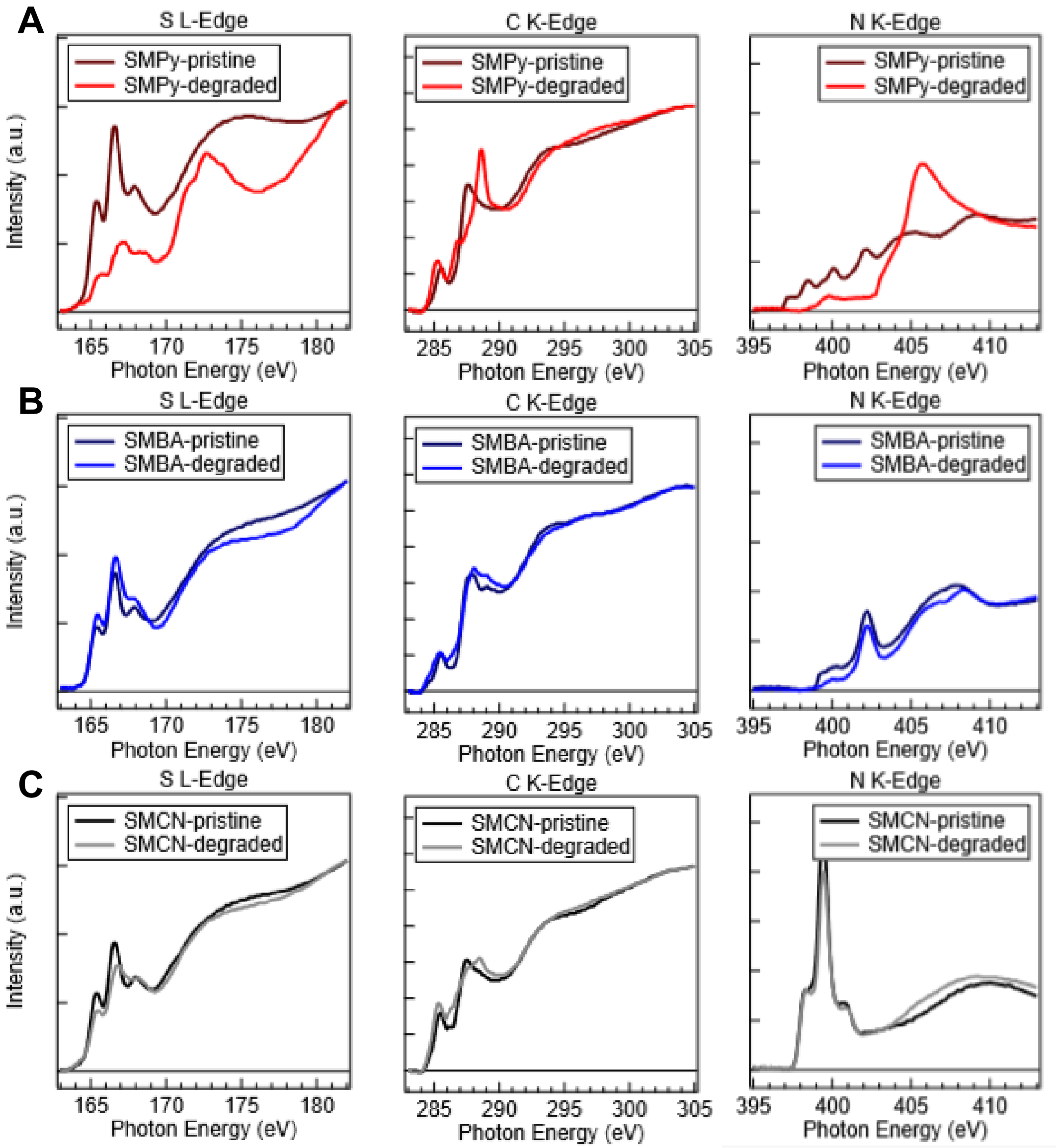

Figure S21. NEXAFS spectra of the S L-edge, C K-edge, and N L-edge for pristine and degraded A) SMPy, B) SMBA and C) SMCN. Neat films stored in a dark glovebox (pristine) or exposed to tungsten halogen array in ambient for 48 hours (degraded).

9. Additional XPS and NEXAFS data

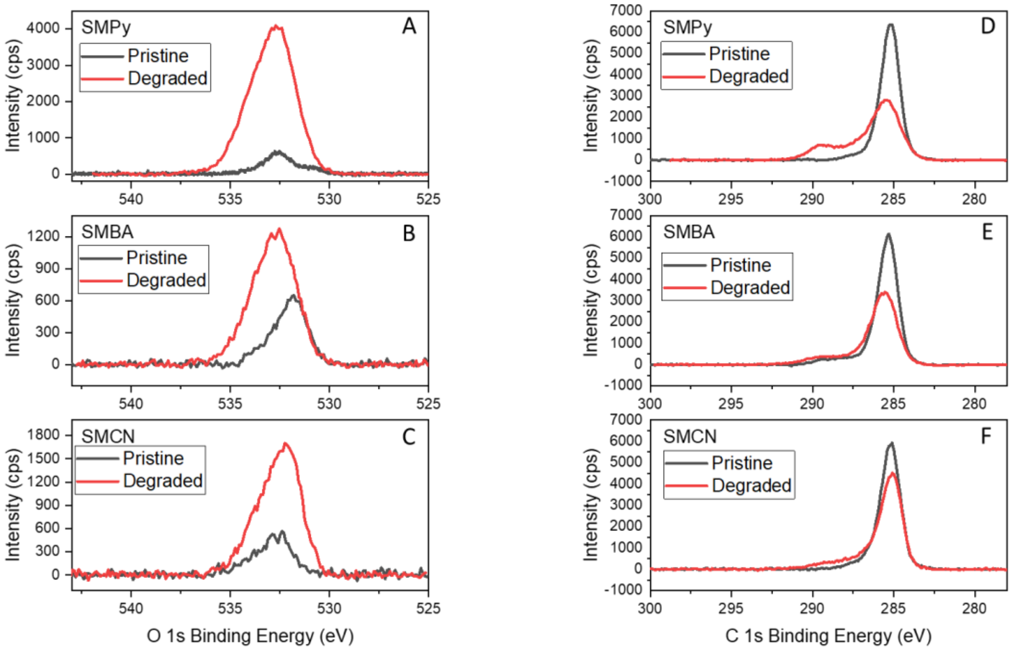

Figure S22. (left)O 1s core level spectra for pristine (black) and degraded (red) films of (A) SMPy (B) SMBA and (C) SMCN. (right) C 1s core level spectra for pristine (black) and degraded (red) of (D) SMPy (E) SMBA and (F) SMCN.

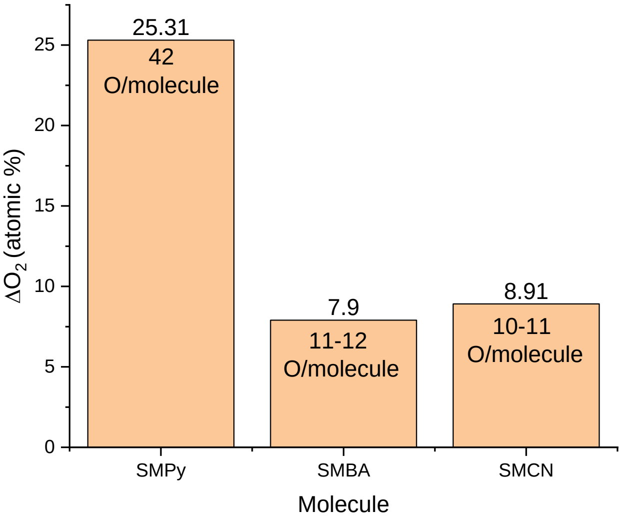

Figure S23. Change in O_2 atomic % of each molecule after degradation conditions relative to pristine film. Oxygen incorporation per molecule is based on the number of oxygen atoms that must be included into the structure of the molecule in order to reach the observed change.

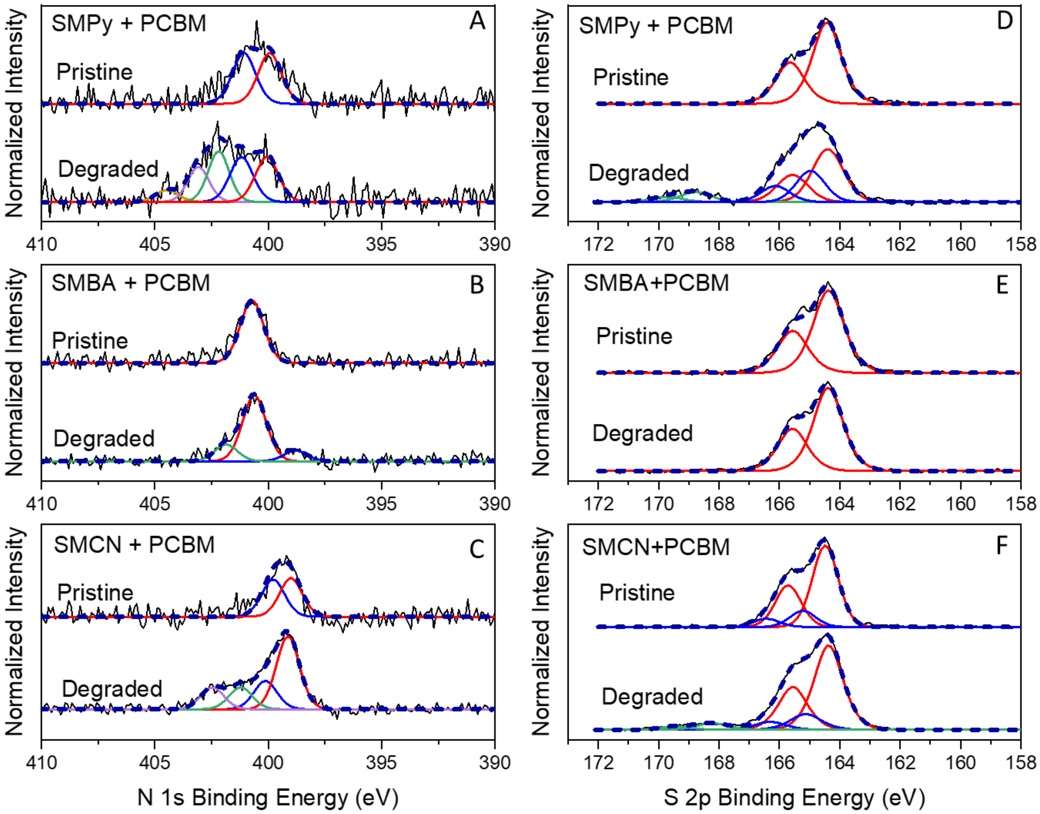

Figure S24. Comparison of XPS changes for OSC: $PC_{71}BM$ 1:1 blended films upon degradation

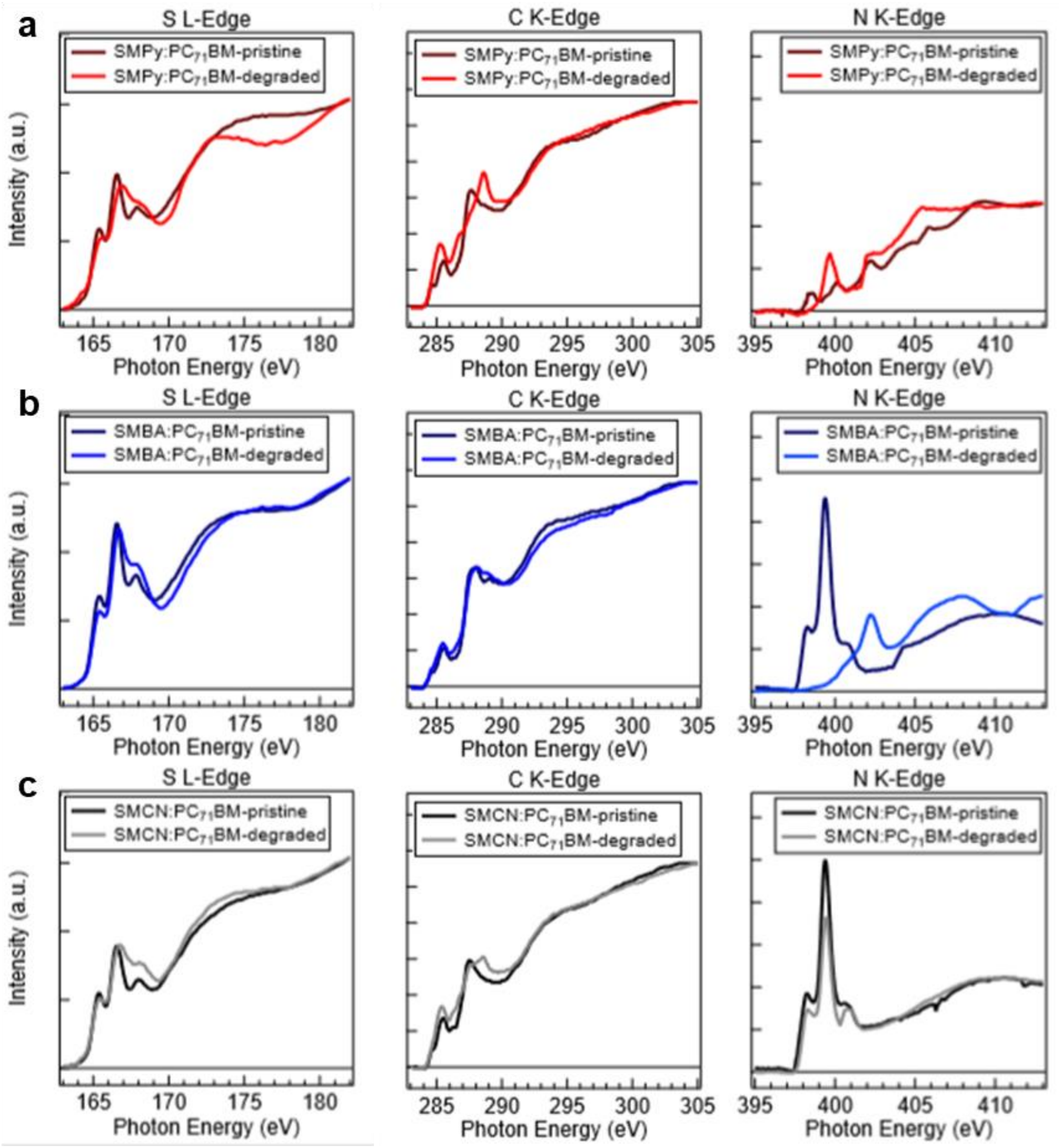

Figure S25. NEXAFS spectra of the S L-edge, C K-edge, and N L-edge for pristine and degraded blends of PC$_{71}$BM and A) SMPy, B) SMBA and C) SMCN. Neat films stored in a dark glovebox (pristine) or exposed to tungsten halogen array in ambient for 48 hours (degraded).

10. References

1. J. Belmar, F. R. Pérez, J. Alderete and C. Zúñiga, *Journal of the Brazilian Chemical Society*, 2005, **16**, 179-189.
2. A. Tang, C. Zhan and J. Yao, *Chemistry of Materials*, 2015, **27**, 4719-4730.
3. S. Helmy, F. A. Leibfarth, S. Oh, J. E. Poelma, C. J. Hawker and J. Read de Alaniz, *Journal of the American Chemical Society*, 2014, **136**, 8169-8172.